*separations*

MDPI

*Article*

# Rapid Discovery of Antimicrobial and Antimalarial Agents from Natural Product Fragments

**Jianying Han [1], Xueting Liu [2], Lixin Zhang [2], Wesley C. Van Voorhis [3], Ronald J. Quinn [1] and Miaomiao Liu [1,*]**

[1] Griffith Institute for Drug Discovery, Griffith University, 170 Kessels Road, Nathan 4111, Qld, Australia; jianying.han@uq.edu.au (J.H.); r.quinn@griffith.edu.au (R.J.Q.)
[2] State Key Laboratory of Bioreactor Engineering, East China University of Science and Technology, Shanghai 200237, China; liuxueting@ecust.edu.cn (X.L.); lxzhang@ecust.edu.cn (L.Z.)
[3] Center for Emerging and Re-emerging Infectious Diseases, Department of Medicine, University of Washington, 750 Republican St., Seattle, WA 98109-4766, USA; wvanvoorhis@medicine.washington.edu
* Correspondence: miaomiao.liu@griffith.edu.au

**Abstract:** Fragment-based drug discovery (FBDD) focuses on small compounds, known as fragments, typically with a molecular weight of less than 300 Da. This study highlights the benefits of employing a pure natural product library for FBDD, contrasting with the predominant use of synthetic libraries. Practical methods for rapidly constructing such libraries from crude extracts were demonstrated across various plant and microbial samples. Twenty-nine (29) natural product fragments, including a new compound (**20**), were identified. Antimicrobial activities were assessed for a subset of the isolated compounds, revealing potent fragments (MICs 4–8 μg/mL) against *Mycobacterium bovis* bacille Calmette-Guérin (BCG), *Staphylococcus aureus* (SA), and methicillin-resistant *S. aureus* (MRSA). Furthermore, a native mass spectrometry technique was introduced to rapidly identify non-competitive fragments against malarial proteins. As a result, two pairs of non-competitive fragments, lepiotin C (**31**) and 7-amino deacetoxy cephalosporanic acid (**32**) binding to dynein light chain 1, methyl gallate (**33**) and β-santanin (**34**) binding to dUTPase, were identified, serving as promising starting points for developing potent malarial protein inhibitors.

**Keywords:** FBDD; natural products; native MS; malarial proteins

check for updates

**Citation:** Han, J.; Liu, X.; Zhang, L.; Van Voorhis, W.C.; Quinn, R.J.; Liu, M. Rapid Discovery of Antimicrobial and Antimalarial Agents from Natural Product Fragments. *Separations* **2024**, *11*, 194. https://doi.org/10.3390/separations11070194

Academic Editor: Paraskevas D. Tzanavaras

Received: 31 May 2024
Revised: 18 June 2024
Accepted: 20 June 2024
Published: 23 June 2024

**Copyright:** © 2024 by the authors. Licensee MDPI, Basel, Switzerland. This article is an open access article distributed under the terms and conditions of the Creative Commons Attribution (CC BY) license (https://creativecommons.org/licenses/by/4.0/).

## 1. Introduction

The discovery of new small-molecule drugs is underpinned by the search for good quality chemical 'leads'. The discovery of suitable leads can be achieved using high-throughput screening (HTS) of chemical libraries [1,2]. Chemical libraries required to obtain several starting points for chemical probes need to be large (~1 million compounds). Furthermore, when screened against newer or more difficult targets, huge compound libraries sometimes yield few hits [3]. Limiting the molecular weight of the chemical library provides greater interrogation of chemical space and is the principle of fragment-based drug discovery (FBDD) [4]. Rather than screening millions of compounds to find drug-sized starting points, FBDD begins with much smaller collections of compounds. Fragments were initially defined as having a molecular weight of less than 300 Da, a logP of less than three, less than three hydrogen bond donors and less than three hydrogen bond acceptors [5]. As such fragment libraries can be a few thousand molecules, about three orders of magnitude smaller than a typical HTS collection [6], the Reymond group has enumerated the number of all possible 'fragment sized' organic molecules which contain up to 17 non-hydrogen atoms to be around $10^{11}$ [7]. However, estimates of the possible number of larger sized, drug-like molecules, range from $10^{20}$ to $10^{24}$ [8]. These numbers suggest that 1000 fragment-sized molecules should sample chemical space significantly more efficiently than 1,000,000 higher-molecular-weight compounds that are used in an HTS library. It is much easier to generate, maintain, and screen a library of a few thousand fragments than millions of

larger molecules, thus increasing accessible to academic laboratories. Furthermore, because fragments are small and typically soluble, they are likely to have better pharmaceutical properties for further development as potential drugs [9]. There are currently over twenty fragment-derived compounds in clinical trials, and three fragment-derived drugs have been approved by the FDA. Another reason to screen smaller molecules is the concept of 'molecular complexity' that was first introduced by Hann and colleagues [10]. The theoretical basis is that as molecules become more complex, they have more possible interactions with a protein target. This leads to a higher risk of unfavourable interactions, which could negatively affect drug efficacy. Thus, the smaller the molecule, the greater the probability it has of matching part of the binding site, leading to higher hit rates [11].

Natural products (NPs) are well known for their biological relevance, high degree of three-dimensionality, and access to areas of largely unexplored chemical space. They have been a source of drug leads offering greater structural diversity than synthetic compounds. Considering only polyketide metabolites, just over 7000 known structures have led to more than 20 commercial drugs with a "hit rate" of 0.3%, which is much better than the <0.001% hit rate for HTS of synthetic compound libraries [12]. However, the role of NPs in fragment-based drug discovery has yet to reach significant prominence. A recently published review summarizes 86 commercially available fragment libraries, 4 of which possess NP-like properties, but none are directly sourced from natural products [13]. Excluding some studies of virtual analysis of natural product-based scaffold databases, there has been very limited research published in the field of using natural product to investigate fragment-based drug discovery. One big challenge is probably the reliable access and supply, especially with respect to higher plants and marine organisms, that can cause challenges with the initial detection of active compounds as well as the subsequent reproducibility of assays or purification [14]. In this manuscript, we highlight the benefits of using a pure natural product library for fragment-based drug discovery. Analysis of both chemistry diversity as well as biological potential will be presented. We also propose practical procedures to rapidly build pure fragment libraries from crude extracts, tailored to different research objectives. Lastly, screening using native mass spectrometry of the in-house natural product fragment library identified non-competitive fragments against malarial proteins.

## 2. Materials and Methods

### *2.1. General Experimental Procedures*

Nuclear magnetic resonance (NMR) spectra were recorded in dimethyl sulfoxide-$d_6$ (DMSO-$d_6$) ($\delta_H$ 2.50 and $\delta_C$ 39.5) at 25 °C on a Bruker Avance HDX 800 MHz spectrometer equipped with a TCI cryoprobe (Billerica, MA, USA). LC-MS data for fragment isolation were recorded on a Thermo Fisher Ultimate 3000 RS LCMS UHPLC-ISQ Single Quadrupole (Waltham, MA, USA). HRMS data for fragment isolation were recorded on a Bruker maXis II ETD ESI-qTOF (Billerica, MA, USA). Optical rotations were recorded on a JASCO P-1020 polarimeter (10 cm cell) (Hachioji-shi, Tokyo, Japan). An Edwards Instrument Company Bioline orbital shaker was used for extraction. The HPLC systems for fractionation and isolation were a Waters 600 pump (Milford, MA, USA) fitted with a 996-photodiode array detector (PDA) and Gilson FC204 fraction collector (Middleton, WI, USA) and a Thermo Ultimate 3000 with a PDA detector (Waltham, MA, USA). A Phenomenex C18 Monolithic column (5 µm, 4.6 × 100 mm) was used for analytical HPLC; a Thermo Hypersil Gold C18 columns (5 µm, 10 × 250 mm) and a Phenomenex Luna C18 columns (5 µm, 10 × 250 mm) were used for semi-preparative purification. All solvents used for extraction, chromatography, $[\alpha]_D$, and MS were HPLC grade, and $H_2O$ was Millipore Milli-Q PF filtered.

### *2.2. Microbe Material*

The marine actinomycete MS110109 was isolated from a sediment sample collected at a depth of 60 m from the South China Sea, China. The endophytes ES120055 and

ES120127 were isolated from Traditional Chinese Medicines (TCMs) *Astilbe rivularis* and *Cirsium shansiense*, respectively, which were originally collected from Yunnan Province, China. The actinomycete LS120194 was isolated from a desert sample collected from Taklimakan Desert.

The identification of the four strains was performed based on the morphological and 16S ribosomal DNA (rDNA) analyses. Multiple sequence alignments with 16S sequences of related species were carried out using CLUSTAL W [15]. A phylogenetic tree was constructed using the neighbor-joining method, as implemented in MEGA 5.0 [16]. Bootstrap values were generated by resampling 1000 replicates. The nucleotide sequences of the 16S rRNA gene have been deposited in GenBank (MS110109: PP320405; ES120055: PP506466; ES120127: PP320412; LS120194: PP320409). The voucher specimen has been deposited at Dr. Zhang's Laboratory, East China University of Science and Technology (strain no. MS110109, ES120055, ES130127, and LS120194).

### *2.3. TCM Material*

The TCMs Huangqi (*Astragalus mongholicus*) and Danshen (*Salvia miltiorrhiza*) were purchased from a Chinese medicine clinic at Brisbane, Australia (Beijing Tong Ren Tang Australia–Brisbane store).

### *2.4. Malarial Fragments*

Fragments **30**–**33** and **35** were purchased from Vitas-M Laboratory (Champaign, IL 61820, United States). Fragment **34** was purchased from Sigma-Aldrich (St. Louis, MO, United States). Fragment **36** was sourced from the in-house Quinn-Liu natural product library.

### *2.5. Malarial Proteins*

Four proteins from *P. falciparum* were expressed in *Escherichia coli*. In general, genes were cloned into expression vectors that enabled tagging of the corresponding proteins with an N-terminal 6-histidine tag, as previously described [17,18]. Proteins were purified using a nickel column (immobilized metal affinity chromatography, IMAC), followed by size exclusion chromatography, concentrated, flash frozen, stored at −80 °C, and shipped on dry ice.

### *2.6. Fermentation, Extraction of the 4 Microbes*

Strains were cultivated on ISP2 agar plates at 28 °C for 7 days. A 250 mL Erlenmeyer flask containing 40 mL of ISP2 liquid medium (1 L: yeast extract 4.0 g, malt extract 10.0 g, dextrose 4.0 g, pH 7.2) was inoculated with each strain and incubated at 28 °C (220 rpm) for 48 h. Aliquots (2 mL) of the pre-culture were used to inoculate 4 × 250 mL Erlenmeyer flasks, each containing 40 mL of ISP2 liquid medium, and the flasks were incubated at 28 °C (220 rpm) for 3 days. Aliquots (2 mL) of the seed cultures were aseptically transferred to 100 × 250 mL Erlenmeyer flasks, each containing 40 mL of media for 7 days.

The broths were then combined and centrifuged to yield a supernatant and a cell pellet of each strain. Supernatant samples were dissolved in 750 mL water and extracted three times with 750 mL n-butanol to give supernatant crude extracts.

### *2.7. Extraction of the 2 TCMs*

The ground and freeze-dried Huangqi (*A. mongholicus*) (10 g) and Danshen (*S. miltiorrhiza*) (10 g) were extracted with 95% ethanol (3 × 300 mL) overnight at room temperature (rt) to afford crude extract.

### *2.8. Fragment Isolation*

Then, 2 g of the supernatant crude extracts of the three bacteria and crude extracts of the two TCM were fractionated using a Sephadex LH-20 column (column volume 200 mL). Sixty fractions (1–60) were collected by eluting with 100% MeOH, with each containing

10 mL of eluate. Each set of five fractions was combined and analyzed by LC-MS to identify the pool fractions containing small fragments with a molecular weight < 300 Da. Individual fractions within the target pool were then validated for fragment composition using LC-MS. Based on the LC-MS and $^1$H NMR profiles, fractions containing fragments were combined and further purified by HPLC.

### *2.9. Biological Assays*

The *M. bovis* bacille Calmette-Guérin (BCG) 1173P2 strain was transformed with green fluorescent protein (GFP) constitutive expression plasmid pUV3583c with direct readout of fluorescence as a measure of bacterial growth. BCG was grown at 37 °C to mid log phase in Middle brook 7H9 broth (Becton Dickinson) supplemented with 10% OADC enrichment (Becton Dickinson, Franklin Lakes, NJ, United States) 0.05% tween-80 and 0.2% glycerol, which then adjusted to $OD_{600}$ = 0.025 with culture medium as bacterial suspension. Aliquots (80 µL) of the bacterial suspension were added to each well of the 96-well microplates (clear flat-bottom), followed by adding compounds (2 µL in DMSO), which were serially twofold diluted. Isoniazid served as positive control and DMSO as negative control. The plate was incubated at 37 °C for 3 days, and GFP fluorescence was measured with Multi-label Plate Reader using the bottom read mode, with excitation at 485 nm and emission at 535 nm. MIC is defined as the minimum concentration of drug that inhibits more than 90% of bacterial growth reflected by fluorescence value.

Antimicrobial assays were performed according to the Antimicrobial Susceptibility Testing Standards outlined by the Clinical and Laboratory Standards Institute (CLSI) (NCCLS 1999) using the bacteria *Staphylococcus aureus* (ATCC 6538), methicillin-resistant S. aureus (MRSA), *Bacillus subtilis* (ATCC 6633), and Pseudomonas aeruginosa (PAO1). For each organism, a loopful of glycerol stock was streaked on an LB agar plate and incubated overnight at 37 °C. A single bacterial colony was picked and suspended in Mueller-Hinton Broth to approximately $1 \times 10^4$ CFU/mL. A twofold serial dilution of each compound to be tested (4000 to 31.25 µg/mL in DMSO) was prepared, and an aliquot of each dilution (2 µL) was added to a 96-well flat-bottom microtiter plate (Greiner, Kremsmünster, Austria). Vancomycin and ciprofloxacin were used as positive controls and DMSO as the negative control. An aliquot (78 µL) of bacterial suspension was then added to each well (to give final compound concentrations of 100 to 0.78 µg/mL in 2.5% DMSO), and the plate was incubated at 37 °C aerobically for 16 h. Finally, the optical density of each well at 600 nm was measured with an EnVision 2103 Multi-label Plate Reader (Perkin-Elmer Life Sciences, Waltham, MA, United States). MIC values were defined as the minimum concentration of compound that inhibited visible bacterial growth.

All experiments were performed in triplicate.

### *2.10. Native MS Experiment*

Each protein was exchanged into ammonium acetate (50 mM, pH 7.3) using size exclusion chromatography (Nalgene NAP-5 size G25, GE Healthcare, Waukesha, WI, United States) prior to native MS analysis. The final concentration of each protein was 10 µM.

Each fragment was dissolved in MeOH at various concentrations. For each injection, 1 µL of fragment dissolved in MeOH was incubated with 49 µL of protein (10 µM) for 1 h at room temperature. Each sample was then injected and analyzed by native MS using the conditions and parameters provided below.

All native MS experiments were performed on a Bruker SolariX XR 12T Fourier transform ion cyclotron resonance mass spectrometer (Bruker Daltonics Inc., Billerica, MA, United States). The ESI source was operated in the direct injection configuration with the use of a 500 µL Hamilton syringe on the built-in syringe pump at a flow rate of 120 µL/h. The capillary voltage was set at 4000 V, and the end-plate voltage was set at −500 V. The dry gas flow rate was 4 L/min, and the temperature was 200 °C. The voltages of the source optics including capillary exit, deflector plate, funnel 1, and skimmer 1 were set at 200, 220,

150, and 30 V, respectively. The optical transfer was set at 2 MHz with a time of flight (TOF) of 1.5 ms. Mass spectra were recorded in positive ion and profile modes with a mass range from 50 to 6000 $m/z$. Each spectrum was a sum of 16 transients (scans) composed of 1 M data points. All aspects of pulse sequence control and data acquisition were controlled by Solarix control software 5.2 in a Windows operating system.

## 3. Results and Discussion

### *3.1. Developing a Drug-Like Natural Product Fragment Library: Extraction*

To obtain a high-quality pure natural product fragment library, several factors should be considered such as the cost, time and resources needed for production. The goal was to achieve the highest quality library possible at a moderate cost and within a reasonable time. Therefore, a multi-step process for creating our pure fragment library from plants and microorganisms was developed and optimized.

As we reported previously, solid-phase extraction (SPE) with hydrophilic–lipophilic balance (HLB) polymer, the divinylbenzene-co-N-vinylpyrrolidone (DVB-co-NVP), by multiple solvent systems (hexane-DCM-MeOH) was developed as an effective method to obtain crude extracts that contain components with log $p < 5$ [19]. We sought to simplify this process with considerations of selectivity, solubility, cost and safety. Both boiling water extraction and alcohol extraction of Traditional Chinese Medicines (TCMs) have been used for over a thousand years in China. The same level of extraction efficacy and bioactive constituents was obtained with these two extraction systems. However, the use of boiling water extraction may have had an effect on the active chemicals through the heating process. It is no doubt that ethanol extraction is much easier and more economically friendly to conduct in laboratory. Furthermore, ethanol is the most common bio-solvent and can be obtained by the fermentation of sugar-rich materials such as sugar beet and cereals [20]. Although it is flammable and potentially explosive, ethanol is used on a large scale because it is easily available in high purity, it has a low price, and it is completely biodegradable. Figure S1 shows the comparison of NMR fingerprints acquired from our previous extraction procedure (DCM-MeOH-SPE) and ethanol extraction. It is clear that ethanol can extract almost the same number and quantity of chemicals from the selected material, and thus it was selected as the extraction method to generate crude extracts.

We also investigated a suitable procedure for the extraction of culture supernatants and cell pellets generated from microbial cultures. Only a very limited amount of metabolites were extracted from a supernatant sample with the (DCM-MeOH-SPE) protocol. One possible reason for the low recovery was considered to be the poor solubility of the supernatant samples since they were directly dried from fermentation broths. To improve the solubility of samples, a liquid-phase extraction process before conducting HLB extraction was used. The supernatant sample was dissolved in 7.5 mL water and extracted three times with 7.5 mL n-butanol. A further HLB extraction was then applied and NMR spectra of crude extracts and HLB eluents showed nearly no differences; therefore, the extraction of supernatant samples with n-butanol only was selected as the extraction method in this project. The extraction effects of solid and liquid extraction methods on cell pellet samples were evaluated. The cell pellet samples were extracted with an equal volume of acetone, a widely used solvent known for effectively breaking down bacterial cell walls and efficiently extracting most secondary metabolites [21,22].

Using the optimized protocol, four microorganisms and two TCMs were processed to obtain crude extracts for further generation of fragments. The criteria for selecting the natural products in this study included the known diversity of small molecules produced by the sources and their potential to yield unique bioactive fragments. Specifically, the selection aimed to cover a broad range of ecological niches to maximize chemical diversity. The selected four microorganisms include MS110109, identified from a marine environment, which is rich in unique microorganisms that produce a wide array of bioactive compounds; two endophytic strains (ES120055 and ES130127), which live inside plant tissues and often produce novel compounds to protect their host plants from pathogens; and a desert strain

(LS120194), which is adapted to extreme conditions and has high potential to synthesize a wide variety of secondary metabolites with unique structures and activities. Two TCMs, Huangqi and Danshen, are known to produce a range of bioactive small molecules, making them excellent candidates for fragment generation. This strategy ensures a broad and representative sampling of chemical space, which is critical for the success of fragment-based drug discovery.

### *3.2. Developing a Drug-Like Natural Product Fragment Library: Purification*

Generating a standard approach applicable to all natural product extracts is challenging due to the inherent diversity of compounds, each possessing different physico-chemical properties. This study aimed to explore the potential of a few commonly used purification methods, with the primary objective of rapidly identifying fragment-sized natural products. We utilized size exclusion chromatography (SEC) followed by LC-MS analysis of each SEC fraction. Specific fractions with fragment-sized compounds were then identified and selected for further purification.

Fifty milligrams of the SEC fractions underwent HPLC and was separated using an Onyx C18 column. Each peak of interest in the HPLC chromatogram was collected in a test tube, dried, and subsequently analyzed by NMR for structure elucidation. In some cases, only one round of HPLC was sufficient to obtain pure compounds. However, multiple rounds of HPLC separation were necessary for purifying Sephadex fractions containing a higher diversity of small molecules (Figure S3). By applying the developed separation protocol, 19 fragment-sized natural products were identified from four actinomycetes, including **1**–**3** isolated from a marine strain *Streptomyces* sp. MS110109, **4**–**7** isolated from an endophyte strain *Streptomyces* sp. ES120055, **8**–**14** isolated from an endophyte strain *Streptomyces* sp. ES130127, and **15**–**19** isolated from a desert strain *Streptomyces* sp. LS120194 (Figure 1). Multiple rounds of HPLC were required to purify compounds **8**, **11**, **17,** and **18**.

Plants in general produce more compounds than actinomycetes (under a single culture condition). In this study, we used two well-known TCMs, Huangqi (*Astragali radix*) and Danshen (*Salvia miltiorrhiza*), recognized for producing a large number of compounds, including a substantial number of small molecules, to test the potential of this Sephadex-HPLC approach [23,24]. The main pharmaceutical effect of Huangqi lies in its potent immunomodulatory activity, enhancing the body's immune response and promoting overall vitality [25]. Rich in bioactive compounds, Huangqi's chemical composition includes saponins, flavonoids, and polysaccharides [26]. These constituents contribute to its anti-inflammatory, antioxidant, and adaptogenic effects, making Huangqi a valuable herb in TCM formulations aimed at boosting immune function, supporting cardiovascular health, and combating stress-related ailments [26]. The fragment-containing fraction obtained from Huangqi showed a more complex composition compared to microbial fractions (Figure S4). Through optimization of the HPLC conditions, six fragments were successfully purified, including one new compound **20** and five known flavonoids **21**–**25** (Figure 1).

Compound **20** was isolated as white powder, with a molecular formula of $C_{14}H_{17}NO_5$ with seven double bond equivalents (DBE), as determined by HRESIMS data on the $[M + H]^+$ ion at *m/z* 280.1183 (calcd for $C_{14}H_{18}NO_5^+$, 280.1179). In the $^1$H NMR spectrum acquired in dimethyl sulfoxide-$d_6$ (DMSO-$d_6$), characteristic signals of a phenyl group were observed, including a downfield pair of triplets at $\delta_H$ 7.34 ppm (2H, t, $J$ = 7.6 Hz) and $\delta_H$ 7.29 ppm (1H, t, $J$ = 7.6 Hz), as well as a doublet at $\delta_H$ 7.23 ppm (2H, d, $J$ = 7.6 Hz). Further analysis of the 1D and 2D NMR spectra (Table 1) revealed the presence of phenylalanine in the structure. The $^{13}$C spectrum exhibited two additional carbonyl signals at $\delta_C$ 168.1 and 166.9 ppm, suggesting their potential attachment to N or O due to their upfield chemical shifts. Both carbons were identified by an HMBC correlation from a singlet methylene ($\delta_H$ 3.35 ppm, $\delta_C$ 41.6 ppm), indicating a carboxyacetyl group in the structure. Finally, an oxygenated methylene ($\delta_H$ 4.09 ppm, $\delta_C$ 60.7 ppm) connected to a methyl group ($\delta_H$ 1.19 ppm, $\delta_C$ 14.0 ppm) was determined to be attached to the carboxyacetyl group based on a key HMBC correlation from the oxygenated methylene protons to the more upfield

carbonyl. Thus, the structure of compound **20** was identified as (3-ethoxy-3-oxopropanoyl)-*D*-phenylalanine (Figure 2). The absolute configuration was determined by comparing the $[\alpha]^{24}_{D}$ value with the literature [27].

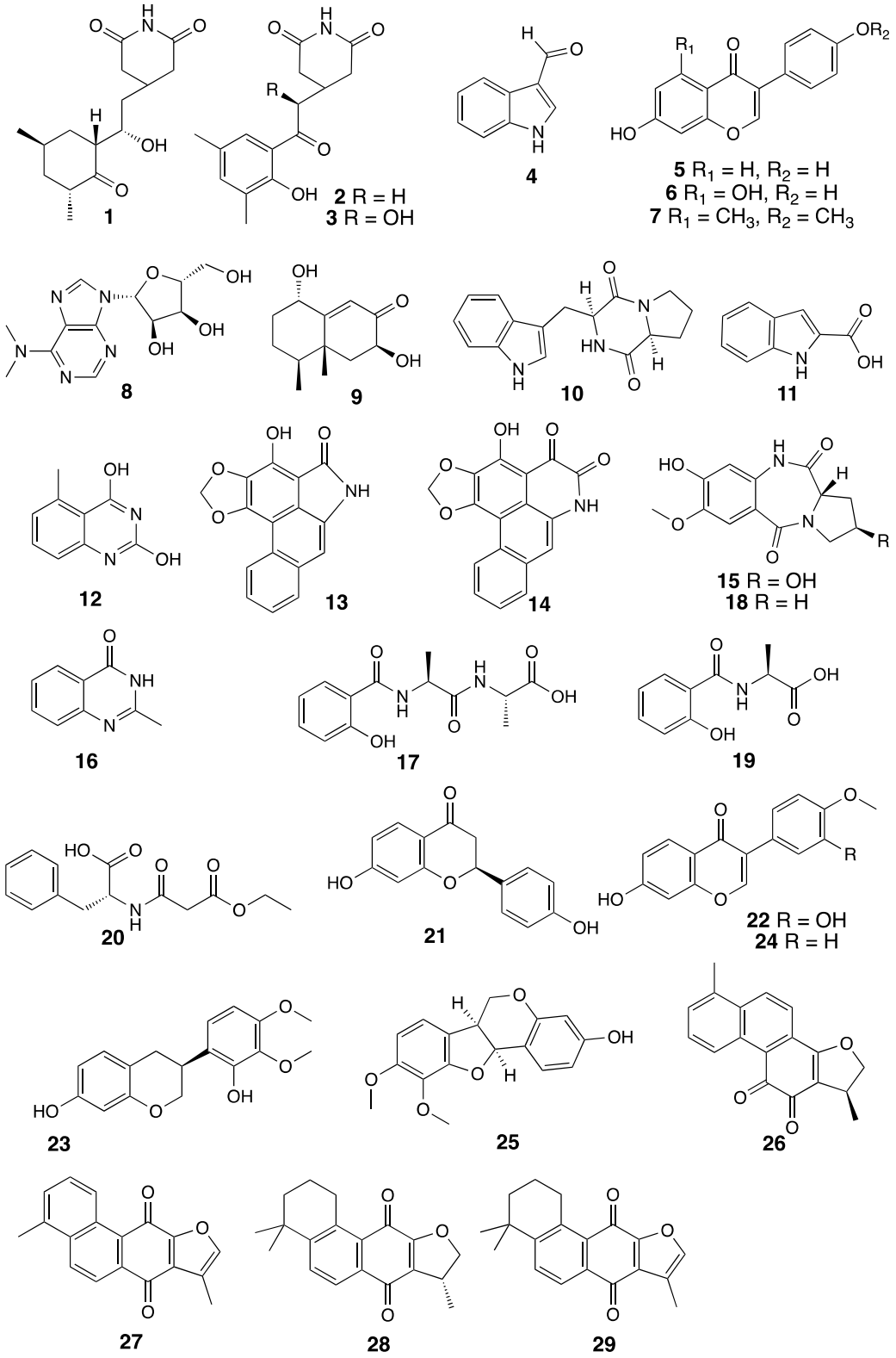



**Figure 1.** Structures of isolated fragments **1**–**29**.

**Table 1.** NMR data of compound **20** in DMSO-$d_6$ at 800 MHz.

| Pos. | $\delta_C$, Type | $\delta_H$, *mult* (*J* in Hz) | COSY | HMBC |
|---|---|---|---|---|
| 1 | 134.8, C | | | |
| 2 | 129.5, CH | 7.26, *d* (7.6) | 3 | 4, 6, 7 |
| 3 | 128.6, CH | 7.34, *t* (7.6) | 2, 4 | 1, 5 |
| 4 | 127.3, CH | 7.29, *t* (7.6) | 3, 5 | 2, 6 |
| 5 | 128.6, CH | 7.34, *t* (7.6) | 4, 6 | 1, 3 |
| 6 | 129.5, CH | 7.26, *d* (7.6) | 5 | 2, 4, 7 |
| 7 | 35.9, $CH_2$ | 3.09, *t* (6.1) | 8 | 1, 2, 6, 8, 9 |
| 8 | 53.2, CH | 4.19, *m* | 7 | |
| 9 | 170.5, C | | | |
| 10 | 168.1, C | | | |
| 11 | 41.6, $CH_2$ | 3.35, *s* | | 10, 12 |
| 12 | 166.9, C | | | |
| 13 | 60.7, $CH_2$ | 4.09, *q* (7.1) | 14 | 12, 14 |
| 14 | 14.0, $CH_3$ | 1.19, *t* (7.1) | 13 | 13 |

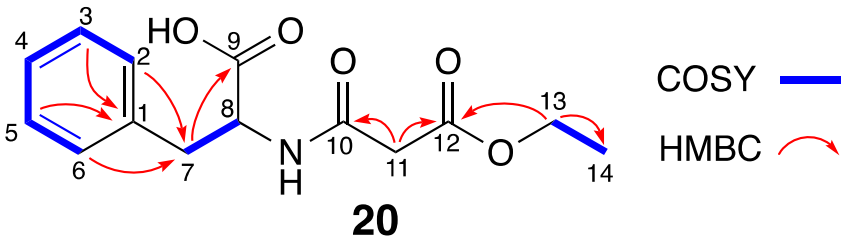



**Figure 2.** Structure of the new fragment **20**.

Danshen, or *S. miltiorrhiza*, is a TCM known for its prominent cardiovascular benefits [28]. One of its main pharmaceutical effects is attributed to its ability to promote blood circulation and alleviate conditions related to cardiovascular health [29]. The main active compounds in Danshen include tanshinones and salvianolic acids, which exhibit antioxidant, anti-inflammatory, and vasodilatory properties [30]. These bioactive components contribute to Danshen's therapeutic potential in treating cardiovascular ailments and supporting overall heart health [30]. By applying the Sephadex-HPLC approach, four major tanshinones namely dihydrotanshinone (**26**), isotanshinone I (**27**), isocryptotanshinone (**28**), and isotanshinone IIA (**29**) were isolated and added to the natural product fragment library.

To evaluate the chemical diversity of the natural product fragments obtained and compare it with traditional synthetic fragment libraries, we utilized ChemGPS-NP, a web-based tool specifically designed for analyzing the chemical diversity found in natural products research (Figure 3) [31]. ChemGPS-NP defines chemical space based on various molecular properties, including size, shape, lipophilicity, polarity, polarizability, flexibility, rigidity, and hydrogen bond capacity [32]. Figure 3 illustrates the chemical space occupied by each compound collection, represented by the extreme values of compounds along the three most significant principal components (PCs), which account for 71% of the variance. These PCs can be interpreted as follows: PC1 represents size, shape, and polarizability; PC2 corresponds to aromatic and conjugation-related properties; PC3 describes lipophilicity, polarity, and hydrogen bond capacity [32]. The natural product fragments (compounds **1–29**) demonstrate a comparable level of chemical diversity to a reported fragment library containing 4733 fragments that was combined from fragment screens against 10 unrelated protein targets [33]. This analysis highlights the broad spectrum of chemical properties present in the natural product fragments.

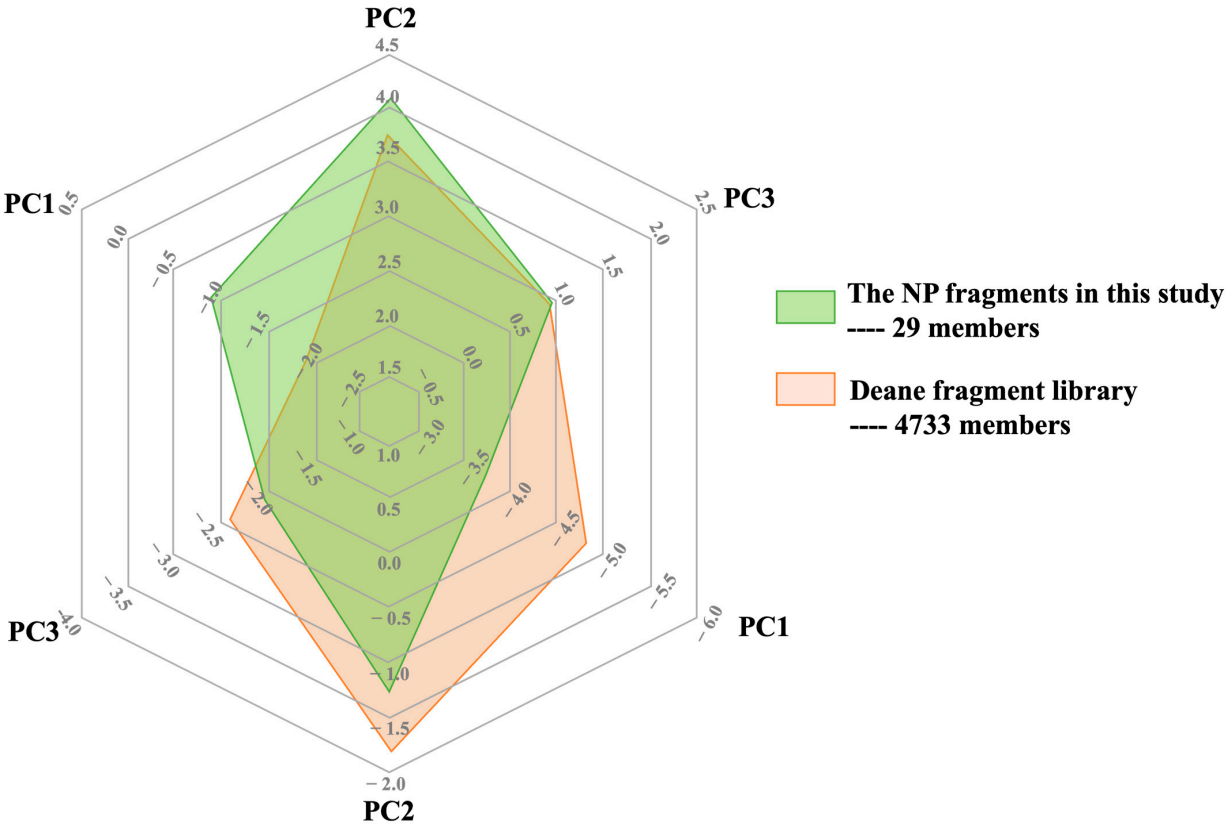



**Figure 3.** Chemical diversity analysis of the natural product fragments **1–29** and a reported 4733-membered fragment library by ChemGPS-NP. Chemical space occupied by each fragment library is represented by the area linked with the extreme values of compounds in the first three principal components (PCs): PC1 (molecular size) versus PC2 (molecular aromaticity) versus PC3 (molecular lipophilicity). Specifically, the extreme values for PC1-PC3 of the 29 natural product fragments in this study and the Deane fragment library are −3.77 to −0.92, −1.28 to 4.09, −2.04 to 0.95 and −4.85 to −1.91, −1.79 to 3.78, −2.45 to 0.92, respectively (Table S1).

### *3.3. Developing a Drug-Like Natural Product Fragment Library: Bioactivity Evaluation*

In an FBDD project, evaluating the biological activity of fragments is a critical step in identifying potential drug candidates. Various methods are developed to assess the biological activity of fragments, aiming to evaluate their cellular inhibition, particularly identify their binding affinity and specificity towards target proteins [34]. Biophysical techniques such as NMR spectroscopy and surface plasmon resonance (SPR) provide insights into fragment–protein interactions, enabling the determination of binding constants and thermodynamic parameters [35]. X-ray crystallography offers high-resolution structural information, elucidating the arrangement of fragments within the target binding site [36]. Additionally, biochemical assays, including enzymatic assays and thermal shift assays, assess the functional impact of fragments on target proteins [37].

The antimicrobial activity of natural product fragments **1–19** was assessed against a range of pathogenic microorganisms (Table 2). Out of the 19 fragments examined, 4 demonstrated significant biological activity against *M. bovis* bacille Calmette-Guérin (BCG) or *S. aureus* (SA), with minimum inhibitory concentration (MIC) values ranging from 4 to 100 μg/mL. Notably, fragments **10** and **13** retained their efficacy even against a methicillin-resistant *S. aureus* (MRSA) strain. In contrast, fragment **14** exhibited comparable inhibition to fragment **13** against the drug-sensitive SA strain but lost its inhibitory effect against the drug-resistant MRSA strain. These findings offer valuable structure-activity relationship (SAR) insights for future development.

**Table 2.** Antimicrobial activities of compounds **1**–**19** *.

| Organism (Strain) | Minimum Inhibitory Concentration (μg/mL) | | | | |
|---|---|---|---|---|---|
| | **3** | **10** | **13** | **14** | **Control** |
| Bacillus Calmette-Guérin (Pasteur 1173P2, BCG) | 100 | 4 | 8 | 8 | 0.37 [a] |
| *Staphylococcus aureus* (ATCC 6538) | NA # | 8 | 8 | 8 | 0.7 [b] |
| Methicillin-resistant *S. aureus* (Clinical strain of Chaoyang hospital) | NA | 8 | 8 | NA | 0.7 [b] |
| *Bacillus subtilis* (ATCC 6633) | NA | NA | NA | NA | 0.35 [b] |
| *Pseudomonas aeruginosa* (PAO1) | NA | NA | NA | NA | 3 [c] |

* Only compounds with observed activity were listed. [a] isoniazid [b] vancomycin [c] ciprofloxacin # NA: not active at 100 μg/mL.

### *3.4. Developing a Drug-Like Natural Product Fragment Library: Protein Binding*

Typically, fragments bind to most target binding sites with an equilibrium dissociation constant (Kd) in the 100s μM to low mM range [38]. This places constraint on the assays that can reliably detect such weak binding and the design of the fragment library (solubility for the high concentrations of fragments needed in assays). Native mass spectrometry (native MS) has been developed as a rapid, sensitive and high throughput method to directly detect protein–ligand interactions [39]. The technique relies on non-denaturing electrospray ionization (ESI) to firstly recognize multi-charged proteins in their near-native states [40]. High-resolution and high mass accuracy measurements, coupled with soft ionization techniques to preserve the integrity of complexes, allow for the determination of ligand mass by measuring the mass of the protein and the mass of the intact protein–ligand complex [41]. In the resulting mass spectrum, the difference between the mass-to-charge ratio for the protein–ligand complex and the unbound protein ions directly affords the molecular weight of the bound ligand. This study used highly purified proteins. However, when dealing with complex biological samples, such as protein mixtures or cell lysates, careful consideration is needed to interpret the results, as native MS detects all molecules in equilibrium, including potential interferences caused by other components in the mixture. Native MS spectra depicting the protein–ligand complex between a malarial protein (P1: CDK-related protein kinase 6 (PK6), PF3D7_1337100 at 10 μM) and a natural product fragment **30** (at 100 μM) are shown below in Figure 4.

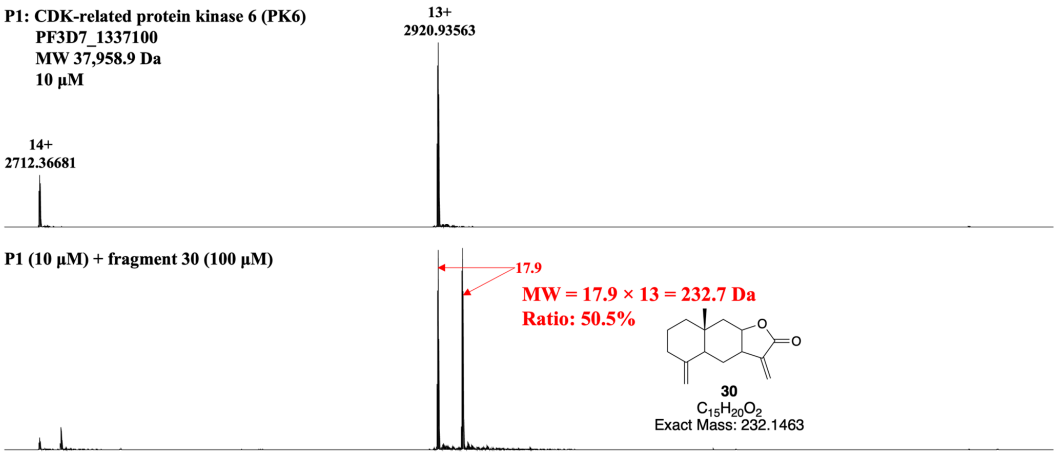



**Figure 4.** Native MS spectra of protein 1 (CDK-related protein kinase 6 (PK6), PF3D7_1337100 at 10 μM) alone (top) and mixed with fragment **30** (isoalantolactone at 100 μM) (bottom). *m/z* values of the major charge states are shown on the spectra.

### *3.5. Developing a Drug-Like Natural Product Fragment Library: Competition Assay*

In a prior investigation, we explored 62 potential protein targets associated with malaria using a natural product-based fragment library [42]. Within this exploration, we identified 96 natural product fragments as binding partners for 32 of the presumed malarial targets. In the current study, we focused on three malarial proteins, each with two binding ligands previously identified in the initial screening. For a FBDD program, identification of the non-competitive ligands that interact with different binding sites on the same protein target is essential for further drug development, e.g., fragment linking [43]. For a specific target, observing two peaks corresponding to two ligand-protein complexes (P + L1) and (P + L2) in a native mass spectrum indicates the binding of the ligand to the same binding site (competitive), while the result (P + L1) + (P + L2) + (P + L1 + L2) shows that L1 and L2 bind to different sites (non-competitive).

Protein 2 dynein light chain 1 (PF3D7_1213600) is a crucial component of the malaria parasite *Plasmodium falciparum*. This protein is responsible for the movement and positioning of cellular organelles, vesicles, and other cargo within the parasite [44]. By disrupting the function of this essential protein, there is promise in impeding the parasite's ability to replicate and cause disease, thus potentially leading to the development of more effective antimalarial drugs. Two fragments, lepiotin C (**31**) and 7-amino deacetoxy cephalosporanic acid (**32**), were initially evaluated individually for their binding affinity to protein 2, with a fragment/protein ratio of 5:1 (Figure 5A). Lepiotin C (**31**) exhibited moderate binding activity with a protein–ligand/total protein ratio of 29.6%, whereas 7-amino deacetoxy cephalosporanic acid (**32**) showed weaker binding to the protein, with a protein–ligand/total protein ratio of 12.1%. Subsequently, both ligands were incubated with the protein simultaneously for a competition mode investigation, with the concentration of fragment **32** increased to 100 μM, resulting in a fragment–fragment–protein ratio of 5:10:1. The resulting mass spectrum revealed binary complexes formed by either fragment with the protein, with fragment **32** forming a higher amount of the complex (26.6%). Remarkably, an intense peak corresponding to the ternary complex formed by both fragments and the protein was detected, with a complex ratio of 27.8%, indicating that fragments **32** and **33** exhibit non-competitive binding to the tested protein.

The malarial protein dUTPase (protein 3, PF3D7_1127100) emerges as a potential drug target due to its crucial role in the replication of the *P. falciparum* parasite [45]. Belonging to the dUTPase enzyme family, it is essential for maintaining nucleotide pool balance by catalyzing the hydrolysis of dUTP to dUMP and pyrophosphate. This enzymatic function is vital for DNA synthesis and repair, making dUTPase an attractive target for antimalarial drug development [46]. Two fragments, methyl gallate (**33**) and $\beta$-santanin (**34**), were assessed for their individual interactions with protein 3, employing a fragment/protein ratio of 5:1 (Figure 5B). Both fragments exhibited comparable binding activities, with protein–ligand/total protein ratios of 22.6% and 18.8%, respectively. Upon simultaneous incubation with the protein, a weak ternary complex representing the binding of both fragments to the protein was observed, with a modest complex ratio of 6.9%. Although the formation of the ternary complex was minimal, it indicates distinct binding sites for fragments **33** and **34** on the protein.

Ubiquitin carboxyl-terminal hydrolase isozyme L3 (UCHL3, PF3D7_1460400), a deubiquitinating enzyme, plays a vital role in the regulation of protein degradation pathways in *P. falciparum* [47]. Specifically, UCHL3 is involved in the removal of ubiquitin molecules from protein substrates, thereby influencing various cellular processes essential for parasite survival and replication [48]. Similarly, two fragments, pyroglutamic acid (**35**) and 3-methoxytryptophan (**36**), were individually investigated for their binding to protein 4 with a fragment/protein ratio of 5:1 (Figure 6). Both fragments exhibited close binding activities to protein 4, with fragment **35** showing a higher protein–ligand complex formation ability (27.3%), while fragment **36** achieved a protein–ligand/total protein ratio of 22.5%. However, when both fragments were incubated with protein 3, only the corresponding

binary complexes were detected. This lack of ternary complex formation indicates that the two fragments compete with each other for the same binding pocket on protein 4.

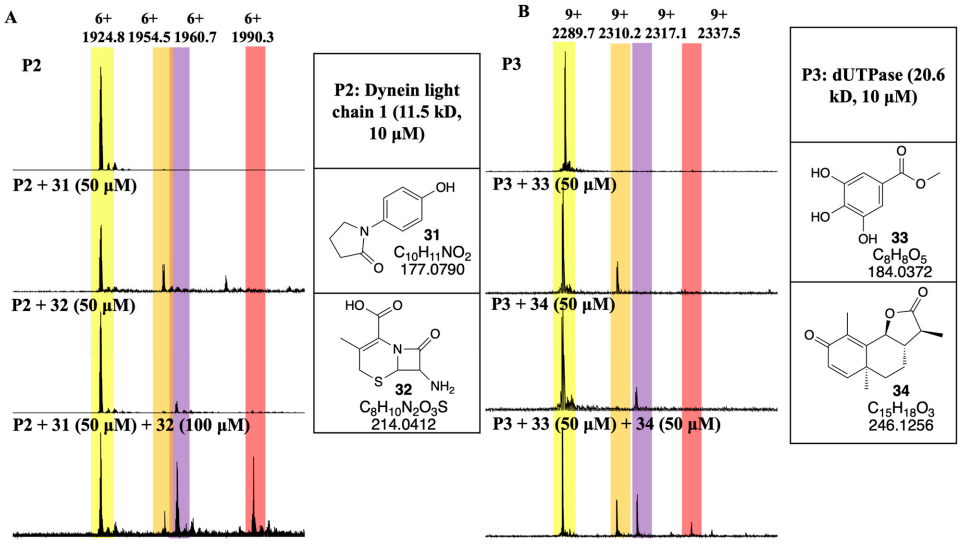



**Figure 5.** Competition study by native MS. (**A**) MS spectra of protein 2 (dynein light chain 1 (PF3D7_1213600) at 10 µM) alone (top), mixed with fragment **31** (lepiotin C at 50 µM) (upper middle), mixed with fragment **32** (7-amino deacetoxy cephalosporanic acid at 50 µM) (upper bottom), and mixed with both fragments **31** (50 µM) and **32** (100 µM). (**B**) MS spectra of protein 3 (dUTPase (PF3D7_1127100) at 10 µM) alone (top), mixed with fragment **33** (methyl gallate at 50 µM) (upper middle), mixed with fragment **34** (*β*-santanin at 50 µM) (upper bottom), and mixed with both fragments **33** (50 µM) and **34** (50 µM). *m/z* values of the major charge states are shown on the spectra.

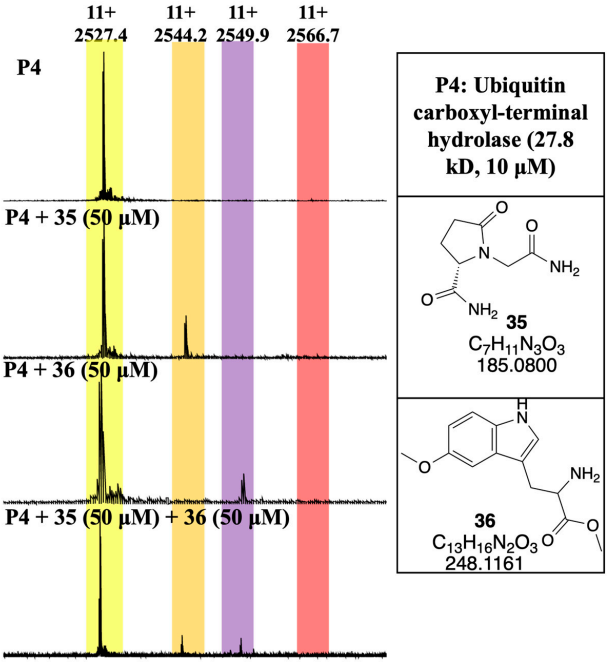



**Figure 6.** Competition study by native MS. MS spectra of protein 4 (ubiquitin carboxyl-terminal hydrolase isozyme L3 (UCHL3, PF3D7_1460400) at 10 µM) alone (top), mixed with fragment **35** (pyroglutamic acid at 50 µM) (upper middle), mixed with fragment **36** (3-methoxytryptophan at 50 µM) (upper bottom), and mixed with both fragments **35** (50 µM) and **36** (100 µM).

## 4. Conclusions

This study outlines a comprehensive process for the development of a natural product fragment library, presenting a promising avenue for fragment-based drug discovery. Through the extraction and purification of natural product fragments from plants and microorganisms, we have showcased the diversity and potential of these compounds in drug discovery. Utilizing a combined chromatography separation platform that starts with a size exclusion separation followed by HPLC purification, we have successfully isolated a range of fragment-sized molecules, including a new natural product (3-ethoxy-3-oxopropanoyl)-*D*-phenylalanine (**20**). The biological evaluation of these microbial fragments (**1**–**19**) against various pathogens highlights their potential as lead compounds for drug development. Compounds **10**, **13**, and **14** showed strong activity, with MICs ranging from 4 to 8 μg/mL against BCG, SA, and MRSA, indicating the therapeutic potential of natural product fragments in combating infectious diseases.

Non-competitive fragments bind to different sites on the same protein, offering a strategic advantage in drug development. By targeting multiple sites on a protein, it is possible to enhance binding affinity and specificity, reduce off-target effects, and overcome resistance mechanisms that might arise with single-site inhibitors. This study identified two pairs of non-competitive fragments, lepiotin C (**31**) and 7-amino deacetoxy cephalosporanic acid (**32**) binding to dynein light chain 1, methyl gallate (**33**) and *β*-santanin (**34**) binding to dUTPase, providing a solid foundation for future drug development. These non-competitive fragments can be further developed into more potent malarial inhibitors through several strategies, such as fragment linking and fragment merging. The unbiased nature of the native MS method ensures that this approach can be applied to a wide range of therapeutic targets and disease areas. As the field of FBDD continues to evolve, the integration of advanced techniques such as native MS will play a crucial role in accelerating the discovery and development of new drugs.

Overall, this study contributes to the growing body of research on fragment-based drug discovery and emphasizes the importance of natural product libraries in this field. By leveraging the rich chemical diversity of natural products, we can accelerate the discovery of novel therapeutics and address unmet medical needs more effectively.

**Supplementary Materials:** The following supporting information can be downloaded at: https://www.mdpi.com/article/10.3390/separations11070194/s1, Figure S1: Comparison of $^{1}$H NMR fingerprints between extraction procedures using DCM-MeOH-SPE (top spectra) and 95% ethanol (bottom spectra). Figure S2: Comparison of $^{1}$H NMR fingerprints between extraction procedures using DCM-MeOH-SPE (top spectra) and n-butanol (bottom spectra). Figure S3: HPLC chromatograms of sephadex fractions from (A). a marine strain *Streptomyces* sp. MS11010, (B). an endophyte strain *Streptomyces* sp. ES120055. Figure S4: HPLC chromatograms of sephadex fractions from TCMs. (A). Huangqi (B). Danshen. Figure S5: $^{1}$H NMR spectrum of **20**. Figure S6: $^{13}$C NMR spectrum of **20**. Figure S7: COSY NMR spectrum of **20**. Figure S8: HSQC NMR spectrum of **20**. Figure S9: HMBC NMR spectrum of **20**. Table S1. Chemical diversity scores PC1 – PC8 for fragments **1**–**29** predicted by ChemGPS-NP.

**Author Contributions:** Conceptualization, M.L.; methodology, J.H. and M.L.; data collection, J.H. and M.L.; writing—original draft preparation, J.H. and M.L.; writing—review and editing, J.H., X.L., L.Z., W.C.V.V., R.J.Q. and M.L.; funding acquisition, M.L. All authors have read and agreed to the published version of the manuscript.

**Funding:** This research was funded by the 2019 Griffith Institute for Drug Discovery Early Career Researcher Grant (Griffith Institute for Drug Discovery, ESK2681) and the 2020 Griffith Sciences New Researcher Grant (Griffith Sciences, ESK2551). M.L. is supported by an National Health and Medical Research Council (NHMRC) Investigator Grant (NHMRC, INV2017517).

**Data Availability Statement:** Data are contained within the article and Supplementary Materials.

**Acknowledgments:** We thank the Open Project Funding of the State Key Laboratory of Bioreactor Engineering, and the Higher Education Discipline Innovation Project (111 Project, No. B18022).

**Conflicts of Interest:** The authors declare no conflicts of interest.

## References

1. Erlanson, D.A.; Fesik, S.W.; Hubbard, R.E.; Jahnke, W.; Jhoti, H. Twenty years on: The impact of fragments on drug discovery. *Nat. Rev. Drug Discov.* **2016**, *15*, 605–619. [CrossRef] [PubMed]
2. Macarron, R.; Banks, M.N.; Bojanic, D.; Burns, D.J.; Cirovic, D.A.; Garyantes, T.; Green, D.V.S.; Hertzberg, R.P.; Janzen, W.P.; Paslay, J.W.; et al. Impact of high-throughput screening in biomedical research. *Nat. Rev. Drug Discov.* **2011**, *10*, 188–195. [CrossRef] [PubMed]
3. Barker, A.; Kettle, J.G.; Nowak, T.; Pease, J.E. Expanding medicinal chemistry space. *Drug Discov. Today* **2013**, *18*, 298–304. [CrossRef] [PubMed]
4. Bohacek, R.S.; McMartin, C.; Guida, W.C. The art and practice of structure-based drug design: A molecular modeling perspective. *Med. Res. Rev.* **1996**, *16*, 3–50. [CrossRef]
5. Congreve, M.; Carr, R.; Murray, C.; Jhoti, H. A rule of three for fragment-based lead discovery? *Drug Discov. Today* **2003**, *8*, 876–877. [CrossRef]
6. Doak, B.C.; Morton, C.J.; Simpson, J.S.; Scanlon, M.J. Design and evaluation of the performance of an NMR screening fragment library. *Aust. J. Chem.* **2013**, *66*, 1465–1472. [CrossRef]
7. Ruddigkeit, L.; van Deursen, R.; Blum, L.C.; Reymond, J.L. Enumeration of 166 billion organic small molecules in the chemical universe database GDB-17. *J. Chem. Inf. Model.* **2012**, *52*, 2864–2875. [CrossRef]
8. Ertl, P. Cheminformatics analysis of organic substituents: Identification of the most common substituents, calculation of substituent properties, and automatic identification of drug-like bioisosteric groups. *J. Chem. Inf. Comput. Sci.* **2003**, *43*, 374–380. [CrossRef]
9. Leeson, P.D.; St-Gallay, S.A. The influence of the 'organizational factor' on compound quality in drug discovery. *Nat. Rev. Drug Discov.* **2011**, *10*, 749–765. [CrossRef]
10. Hann, M.M.; Leach, A.R.; Harper, G. Molecular complexity and its impact on the probability of finding leads for drug discovery. *J. Chem. Inf. Comput. Sci.* **2001**, *41*, 856–864. [CrossRef]
11. Leach, A.R.; Hann, M.M. Molecular complexity and fragment-based drug discovery: Ten years on. *Curr. Opin. Chem. Biol.* **2011**, *15*, 489–496. [CrossRef] [PubMed]
12. Weissman, K.J.; Leadlay, P.F. Combinatorial biosynthesis of reduced polyketides. *Nat. Rev. Microbiol.* **2005**, *3*, 925–936. [CrossRef]
13. Imbernon, J.R.; Jacquemard, C.; Bret, G.; Marcou, G.; Kellenberger, E. Comprehensive analysis of commercial fragment libraries. *RSC Med. Chem.* **2022**, *13*, 300–310. [CrossRef] [PubMed]
14. Li, J.W.H.; Vederas, J.C. Drug discovery and natural products: End of an era or an endless frontier? *Science* **2009**, *325*, 161–165. [CrossRef] [PubMed]
15. Larkin, M.A.; Blackshields, G.; Brown, N.P.; Chenna, R.; McGettigan, P.A.; McWilliam, H.; Valentin, F.; Wallace, I.M.; Wilm, A.; Lopez, R.; et al. Clustal W and clustal X version 2.0. *Bioinformatics* **2007**, *23*, 2947–2948. [CrossRef] [PubMed]
16. Saitou, N.; Nei, M. The neighbor-joining method—A new method for reconstructing phylogenetic trees. *Mol. Biol. Evol.* **1987**, *4*, 406–425. [PubMed]
17. Bajsa, J.; McCluskey, A.; Gordon, C.P.; Stewart, S.G.; Hill, T.A.; Sahu, R.; Duke, S.O.; Tekwani, B.L. The antiplasmodial activity of norcantharidin analogs. *Bioorg. Med. Chem. Lett.* **2010**, *20*, 6688–6695. [CrossRef]
18. Suberu, J.O.; Gorka, A.P.; Jacobs, L.; Roepe, P.D.; Sullivan, N.; Barker, G.C.; Lapkin, A.A. Anti-plasmodial polyvalent interactions in *Artemisia annua* L. aqueous extract—Possible synergistic and resistance mechanisms. *PLoS ONE* **2013**, *8*, e80790. [CrossRef]
19. Camp, D.; Davis, R.A.; Campitelli, M.; Ebdon, J.; Quinn, R.J. Drug-like properties: Guiding principles for the design of natural product libraries. *J. Nat. Prod.* **2012**, *75*, 72–81. [CrossRef]
20. Chemat, F.; Vian, M.A.; Cravotto, G. Green extraction of natural products: Concept and principles. *Int. J. Mol. Sci.* **2012**, *13*, 8615–8627. [CrossRef]
21. Liu, M.M.; Abdel-Mageed, W.M.; Ren, B.; He, W.N.; Huang, P.; Li, X.L.; Bolla, K.; Guo, H.; Chen, C.X.; Song, F.H.; et al. Endophytic *Streptomyces* sp. Y3111 from traditional Chinese medicine produced antitubercular pluramycins. *Appl. Microbiol. Biotechnol.* **2014**, *98*, 1077–1085. [CrossRef] [PubMed]
22. Liu, M.M.; Grkovic, T.; Liu, X.T.; Han, J.Y.; Zhang, L.X.; Quinn, R.J. A systems approach using OSMAC, Log P and NMR fingerprinting: An approach to novelty. *Synth. Syst. Biotechnol.* **2017**, *2*, 276–286. [CrossRef] [PubMed]
23. Fu, J.; Wang, Z.H.; Huang, L.F.; Zheng, S.H.; Wang, D.M.; Chen, S.L.; Zhang, H.T.; Yang, S.H. Review of the botanical characteristics, phytochemistry, and pharmacology of *Astragalus membranaceus* Huangqi. *Phytother. Res.* **2014**, *28*, 1275–1283. [CrossRef] [PubMed]
24. Mei, X.D.; Cao, Y.F.; Che, Y.Y.; Li, J.; Shang, Z.P.; Zhao, W.J.; Qiao, Y.J.; Zhang, J.Y. Danshen: A phytochemical and pharmacological overview. *Chin. J. Nat. Med.* **2019**, *17*, 59–80.
25. Chen, Z.J.; Liu, L.J.; Gao, C.F.; Chen, W.J.; Vong, C.T.; Yao, P.F.; Yang, Y.H.; Li, X.Z.; Tang, X.D.; Wang, S.P.; et al. Astragali Radix (Huangqi): A promising edible immunomodulatory herbal medicine. *J. Ethnopharmacol.* **2020**, *258*, 112895. [CrossRef]

26. Chang, X.N.; Chen, X.F.; Guo, Y.X.; Gong, P.; Pei, S.Y.; Wang, D.N.; Wang, P.P.; Wang, M.R.; Chen, F.X. Advances in chemical composition, extraction techniques, analytical methods, and biological activity of Astragali radix. *Molecules* **2022**, *27*, 1058. [CrossRef] [PubMed]
27. Poncet, J.; Jouin, P.; Castro, B.; Nicolas, L.; Boutar, M.; Gaudemer, A. Tetramic acid chemistry. 1. reinvestigation of racemization during the synthesis of tetramic acids via dieckmann cyclization. *J. Chem. Soc.-Perkin Trans.* **1990**, *1*, 611–616. [CrossRef]
28. Wang, L.L.; Ma, R.F.; Liu, C.Y.; Liu, H.X.; Zhu, R.Y.; Guo, S.Z.; Tang, M.K.; Li, Y.; Niu, J.Z.; Fu, M.; et al. *Salvia miltiorrhiza*: A potential red light to the development of cardiovascular diseases. *Curr. Pharm. Des.* **2017**, *23*, 1077–1097. [CrossRef]
29. Ren, J.; Fu, L.; Nile, S.H.; Zhang, J.; Kai, G.Y. *Salvia miltiorrhiza* in treating cardiovascular diseases: A review on Its pharmacological and clinical applications. *Front. Pharmacol.* **2019**, *10*, 753. [CrossRef]
30. Li, Z.M.; Xu, S.W.; Liu, P.Q. *Salvia miltiorrhiza* Burge (Danshen): A golden herbal medicine in cardiovascular therapeutics. *Acta Pharmacol. Sin.* **2018**, *39*, 802–824. [CrossRef]
31. Rosen, J.; Lovgren, A.; Kogej, T.; Muresan, S.; Gottfries, J.; Backlund, A. ChemGPS-NP(Web): Chemical space navigation online. *J. Comput. Aided Mol. Des.* **2009**, *23*, 253–259. [CrossRef] [PubMed]
32. Larsson, J.; Gottfries, J.; Muresan, S.; Backlund, A. ChemGPS-NP: Tuned for navigation in biologically relevant chemical space. *J. Nat. Prod.* **2007**, *70*, 789–794. [CrossRef] [PubMed]
33. Carbery, A.; Skyner, R.; von Delft, F.; Deane, C.M. Fragment Libraries Designed to Be Functionally Diverse Recover Protein Binding Information More Efficiently Than Standard Structurally Diverse Libraries. *J. Med. Chem.* **2022**, *65*, 11404–11413. [CrossRef] [PubMed]
34. Kirsch, P.; Hartman, A.M.; Hirsch, A.K.H.; Empting, M. Concepts and core principles of fragment-based drug design. *Molecules* **2019**, *24*, 4309. [CrossRef] [PubMed]
35. Price, A.J.; Howard, S.; Cons, B.D. Fragment-based drug discovery and its application to challenging drug targets. *Struct. -Based Drug Des. Insights Acad. Ind.* **2017**, *61*, 475–484.
36. Maveyraud, L.; Mourey, L. Protein X-ray crystallography and drug discovery. *Molecules* **2020**, *25*, 1030. [CrossRef] [PubMed]
37. Coyle, J.; Walser, R. Applied biophysical methods in fragment-based drug discovery. *SLAS Discov.* **2020**, *25*, 471–490. [CrossRef]
38. Liu, M.; Mirza, A.; McAndrew, P.C.; Thapaliya, A.; Pierrat, O.A.; Stubbs, M.; Hahner, T.; Chessum, N.E.A.; Innocenti, P.; Caldwell, J.; et al. Determination of ligand-binding affinity ($K_d$) using transverse relaxation rate ($R_2$) in the ligand-observed $^1$H NMR experiment and applications to fragment-based drug discovery. *J. Med. Chem.* **2023**, *66*, 10617–10627. [CrossRef]
39. Quinn, R.J.; Mak, T.; Littler, D.R.; Rossjohn, J.; Liu, M.M. Discovery of Anti-SARS-CoV-2 Nsp9 Binders from Natural Products by a Native Mass Spectrometry Approach. *J. Nat. Prod.* **2023**, *86*, 2630–2637. [CrossRef]
40. Liu, M.; Littler, D.R.; Rossjohn, J.; Quinn, R.J. Binding studies of the prodrug HAO472 to SARS-Cov-2 nsp9 and variants. *ACS Omega* **2022**, *7*, 7327–7332. [CrossRef]
41. Littler, D.R.; Liu, M.; McAuley, J.L.; Lowery, S.A.; Illing, P.T.; Gully, B.S.; Purcell, A.W.; Chandrashekaran, I.R.; Perlman, S.; Purcell, D.F.J.; et al. A natural product compound inhibits coronaviral replication in vitro by binding to the conserved Nsp9 SARS-CoV-2 protein. *J. Biol. Chem.* **2021**, *297*, 101362. [CrossRef] [PubMed]
42. Vu, H.; Pedro, L.; Mak, T.; McCormick, B.; Rowley, J.; Liu, M.M.; Di Capua, A.; Williams-Noonan, B.; Pham, N.B.; Pouwer, R.; et al. Fragment-based screening of a natural product library against 62 potential malaria drug targets employing native mass spectrometry. *ACS Infect. Dis.* **2018**, *4*, 431–444. [CrossRef] [PubMed]
43. Bancet, A.; Raingeval, C.; Lomberget, T.; Le Borgne, M.; Guichou, J.F.; Krimm, I. Fragment linking strategies for structure-based drug design. *J. Med. Chem.* **2020**, *63*, 11420–11435. [CrossRef] [PubMed]
44. Daher, W.; Pierrot, C.; Kalamou, H.; Pinder, J.C.; Margos, G.; Dive, D.; Franke-Fayard, B.; Janse, C.J.; Khalife, J. *Plasmodium falciparum* Dynein light chain 1 interacts with actin/myosin during blood stage development. *J. Biol. Chem.* **2010**, *285*, 20180–20191. [CrossRef] [PubMed]
45. Kumar, H.; Kehrer, J.; Singer, M.; Reinig, M.; Santos, J.M.; Mair, G.R.; Frischknecht, F. Functional genetic evaluation of DNA house-cleaning enzymes in the malaria parasite: dUTPase and Ap4AH are essential in *Plasmodium berghei* but ITPase and NDH are dispensable. *Expert Opin. Ther. Targets* **2019**, *23*, 251–261. [CrossRef] [PubMed]
46. Pérez-Moreno, G.; Sánchez-Carrasco, P.; Ruiz-Pérez, L.M.; Johansson, N.G.; Müller, S.; Baragana, B.; Hampton, S.E.; Gilbert, I.H.; Kaiser, M.; Sarkar, S.; et al. Validation of *Plasmodium falciparum* dUTPase as the target of 5′-tritylated deoxyuridine analogues with anti-malarial activity. *Malar. J.* **2019**, *18*, 392. [CrossRef]
47. Imhoff, R.D.; Rosenthal, M.R.; Ashraf, K.; Bhanot, P.; Ng, C.L.; Flaherty, D.P. Identification of covalent fragment inhibitors for *Plasmodium falciparum* UCHL3 with anti-malarial efficacy. *Bioorganic Med. Chem. Lett.* **2023**, *94*, 129458. [CrossRef]
48. Artavanis-Tsakonas, K.; Weihofen, W.A.; Antos, J.M.; Coleman, B.I.; Comeaux, C.A.; Duraisingh, M.T.; Gaudet, R.; Ploegh, H.L. Characterization and structural studies of the ubiquitin and nedd8 hydrolase UCHL3. *J. Biol. Chem.* **2010**, *285*, 6857–6866. [CrossRef]


**Disclaimer/Publisher's Note:** The statements, opinions and data contained in all publications are solely those of the individual author(s) and contributor(s) and not of MDPI and/or the editor(s). MDPI and/or the editor(s) disclaim responsibility for any injury to people or property resulting from any ideas, methods, instructions or products referred to in the content.